Evaluation of Multimode Coupled Bridge Response and Equivalent Static Wind Loading

Xinzhong Chen[1]* and Ahsan Kareem[2]

[1] *Assistant Professor of Civil Engineering, Texas Tech University, Texas, USA, xinzhong.chen@ttu.edu*
[2] *Professor of Engineering, University of Notre Dame, Indiana, USA, kareem@nd.edu*

ABSTRACT

This study addresses recent developments on the evaluation of multimode coupled bridge response and modeling of equivalent static wind loading on bridges when subjected to strong winds. First, the coupled bridge flutter is studied with an emphasis placed on the participation of structural modes in flutter, not only based on their amplitudes in flutter motion, but more importantly, by delving into their contributions to flutter modal damping. The bimodal coupled flutter is then revisited based on a framework with closed-form formulations that sheds more insights to the underlying physics of coupled flutter. This discussion was followed by a unified analysis framework of integrating both flutter and buffeting analysis that better points out the roles of both self-excited and buffeting forces on bridge response to wind fluctuations. Finally, the methodology for modeling equivalent static wind loading associated with multimode coupled buffeting is discussed with applications to bridge design.

KEYWORDS: Flutter; Buffeting; Aeoelasticity; Aerodynamics; Wind Load; Bridges; Random Vibration

INTRODUCTION

An increase in the span length of cable-supported bridges leads to a concomitant decrease in their natural frequencies. Consequently, the reduced design wind velocity, which is defined as the ratio of design wind velocity to the bridge frequency and deck width and serves as a non-dimensional measure of strong winds, significantly increases for longer spans. Furthermore, a decrease in bridge weight, damping and frequency ratio between torsional and vertical modes renders long span bridges very vulnerable to strong winds. These facts, coupled with the increased demand on reliability and cost-effectiveness of bridges, makes long span design very challenging. This challenge calls for improved understanding of bridge-wind interaction and development of advanced tools for quantifying bridge response under strong winds. This would help to tailor advanced design of bridges with superior aerodynamic and structural characteristics hence their improved performance.

Evaluation of bridge buffeting and flutter generally requires use of multimode coupled analysis frameworks that facilitate synthesis of information concerning wind climate at the bridge site, aerodynamic forces on the bridge sections, and the finite element model of the entire bridge (e.g., Jones et al. 1998; Matsumoto 1999; Miyata et al. 1999; Chen et al. 2000a and b). Within these frameworks, the flutter analysis is performed through the solution of a complex eigenvalue problem. This analysis not only offers the prediction of critical flutter velocity, but also provides information concerning the influence of self-excited forces on the modal properties as wind velocity increases. That helps in understanding the changes in modal damping and the development of coupled flutter. On the other hand, the buffeting analysis is often conducted in the frequency domain through spectral analysis, while the time domain frameworks are more appropriate for nonlinear problems of either structural or aerodynamic origin, and for bridges under nonstationary wind excitations (Diana et al. 1999; Chen and Kareem 2000b and 2003). The frequency domain buffeting analysis involves the evaluation of complex frequency response matrix (transfer matrix) of aeroelastic bridge system. For a linear system with frequency independent parameters, the transfer matrix is readily expressed in terms of its modal properties. However, it is not the case for an aeroelastic bridge system that involves frequency dependent parameters attributed to unsteady aerodynamic forces. Consequently, the information of modal properties at varying wind velocities predicted through flutter analysis has not yet been explicitly

---

*Corresponding author. Tel: +1-806-742-3476; Fax: +1-806-742-3446
Mailing address: Box 41023, Lubbock, TX 79409-1023, USA

employed in predicting and interpreting buffeting response. As a result, in current analysis frameworks, the predictions of flutter and buffeting have to be treated as two separate procedures without establishing an explicit nexus between them. This practice has limited our ability to better understand the aeroelastic behavior of long span bridges to strong winds.

This study addresses recent developments on the evaluation of multimode coupled bridge response and modeling of equivalent static wind loading on bridges when subjected to strong winds. First, the coupled bridge flutter is studied with an emphasis placed on the participation of structural modes in flutter, not only based on their amplitudes in flutter mode, but more importantly, by delving into their contributions to flutter modal damping. This investigation highlights the important role of the bimodal coupled flutter analysis and section model testing in wind tunnel, consisting of the fundamental vertical and torsional modes. The bimodal coupled flutter is then revisited based on a framework with closed-form formulations that sheds more insights to the underlying physics of coupled flutter. This discussion was followed by a unified analysis framework of integrating both flutter and buffeting analysis that better points out the roles of both self-excited and buffeting forces on bridge response to wind fluctuations. Finally, the methodology for modeling equivalent static wind loading associated with multimode coupled buffeting is discussed with applications to bridge design.

MULTIMODE COUPLED BRIDGE FLUTTER

The equations of bridge motion subjected to wind excitations with the mean wind direction normal to the bridge deck axis can be expressed as follows in terms of the generalized modal coordinates (e.g., Chen et al. 2000a and b):

$$\mathbf{M}\ddot{\mathbf{q}} + \mathbf{C}\dot{\mathbf{q}} + \mathbf{K}\mathbf{q} = \mathbf{Q}_{se} + \mathbf{Q}_b \tag{1}$$

$$\mathbf{M} = \mathrm{diag}[m_j]; \quad \mathbf{C} = \mathrm{diag}[2\xi_{sj}\omega_{sj}m_j]; \quad \mathbf{K} = \mathrm{diag}[m_j\omega_{sj}^2] \tag{2}$$

$$\mathbf{Q}_{se} = \frac{1}{2}\rho U^2\left(\mathbf{A}_s(k)\mathbf{q} + \frac{b}{U}\mathbf{A}_d(k)\dot{\mathbf{q}}\right); \qquad \mathbf{Q}_b = \frac{1}{2}\rho U^2\left(\mathbf{A}_{bu}(k)\frac{\mathbf{u}}{U} + \mathbf{A}_{bw}(k)\frac{\mathbf{w}}{U}\right) \tag{3}$$

where $\mathbf{M}$, $\mathbf{C}$ and $\mathbf{K}$ = generalized mass, damping and stiffness matrices; m_j, ξ_{sj}, and ω_{sj} = jth generalized mass, damping ratio and frequency; $\mathbf{Q}_{se}$ and $\mathbf{Q}_b$ = generalized self-excited and buffeting force vectors; $\mathbf{A}_s(k)$ and $\mathbf{A}_d(k)$ = aerodynamic stiffness and damping matrices, which are functions of flutter derivatives and structural mode shapes; $\mathbf{A}_{bu}(k)$ and $\mathbf{A}_{bw}(k)$ = buffeting force matrices, which are functions of static force coefficients, aerodynamic admittance functions, coherence functions of aerodynamic forces, and structural mode shapes; $\mathbf{u}$ and $\mathbf{w}$ = longitudinal and vertical component vectors of wind fluctuations; ρ = air density; U = mean wind velocity; $B = 2b$ = bridge deck width; $k = \omega b/U$ = reduced frequency; ω = frequency of motion. It is worthy of mention that as $\mathbf{A}_d(k)$ and $\mathbf{A}_s(k)$ are frequency dependent and non-diagonal matrices, the equations of motion of bridge aeroelastic system become frequency dependent and coupled.

The influence of self-excited forces on bridge modal properties at a given wind velocity can be quantified through the solution of the following complex eigenvalue problem (e.g., Chen et al. 2000a):

$$\lambda_j\left\{\begin{array}{c}\mathbf{\Phi}_j \\ \lambda_j\mathbf{\Phi}_j\end{array}\right\} = \left[\begin{array}{cc}\mathbf{0} & \mathbf{I} \\ -\mathbf{M}^{-1}\mathbf{K}_1(k_j) & -\mathbf{M}^{-1}\mathbf{C}_1(k_j)\end{array}\right]\left\{\begin{array}{c}\mathbf{\Phi}_j \\ \lambda_j\mathbf{\Phi}_j\end{array}\right\} \tag{4}$$

$$\mathbf{C}_1(k_j) = \mathbf{C} - \frac{1}{2}\rho Ub\mathbf{A}_d(k_j); \quad \mathbf{K}_1(k_j) = \mathbf{K} - \frac{1}{2}\rho U^2\mathbf{A}_s(k_j) \tag{5}$$

$$\lambda_j = -\xi_j\omega_j + i\omega_j\sqrt{1-\xi_j^2} \tag{6}$$

where λ_j and $\mathbf{\Phi}_j$ = jth complex eigenvalue and eigenmode (mode shape); ω_j and ξ_j = jth complex modal frequency and damping ratio; $k_j = \omega_j b/U$; $i = \sqrt{-1}$.

Fig.1 and 2 show the predicted modal frequencies and damping ratios of a suspension bridge with a center span of nearly 2000 m. The flutter derivatives were calculated using Theodorsen function. The structural mode damping ratio for each mode was assumed as 0.0032. Analyses involving different combinations of

structural modes were conducted where modes 2, 8 and 11 are the first, second and third symmetric vertical bending modes, mode 9 the second symmetric lateral bending mode, and mode 10 the first symmetric torsional mode. The bimodal flutter analysis that involves modes 2 and 8 results in a critical flutter velocity of 68.3m/s, which is very close to 69.3m/s predicted when involving first 15 modes. Considering the curve veering of the frequency and damping loci of the modal branches 9 and 10, the results involving multiple modes are consistent with the bimodal coupled system.
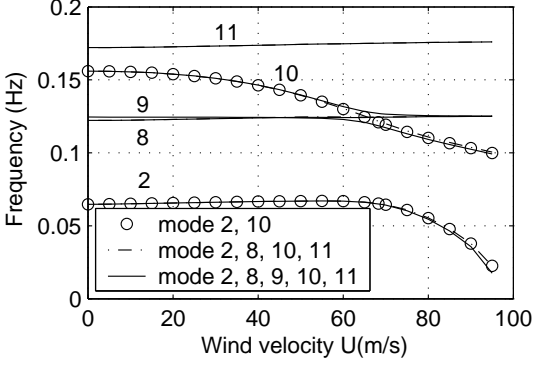
Fig. 1 Modal frequencies at varying wind velocities
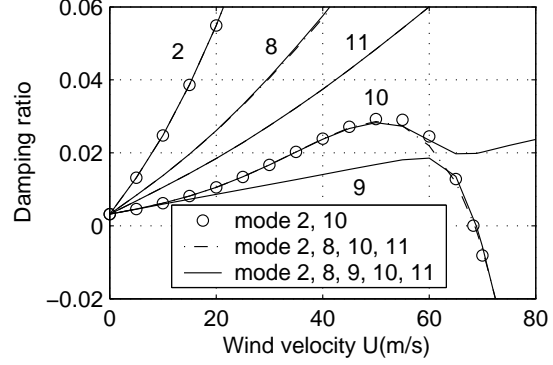
Fig. 2 Modal damping ratios at varying wind velocities

Selection of participating structural modes in a multimode flutter analysis is usually not a difficult issue in practice. In fact, in most cases involving only a few important modes, as demonstrated by the aforementioned example, can provide an adequately accurate estimate of flutter behavior. The significance of structural modes in bridge flutter may be identified through their amplitudes in the flutter motion. However, clarification of their contributions to the damping of flutter mode offers more accurate information regarding the role played by each structural mode in the generation of coupled flutter (Chen et al. 2000a).

The modal damping can be related to the change in system energy during a cycle of vibration. The generalized modal displacement $\mathbf{q}(t)$ in the flutter mode is expressed as

$$\mathbf{q}(t) = \{|\Phi|_i \sin(\omega t + \varphi_i)\} \tag{7}$$

where $|\Phi|_i$ and φ_i = the amplitude and phase angle of ith modal displacement determined through the complex mode shape; ω is the vibration frequency.

The increase in system energy during a cycle of vibration, ΔE, can be expressed by the work done by the generalized aerodynamic forces as (excluding the contribution of the structural damping force):

$$\Delta E = \int_0^{2\pi/\omega} \frac{1}{2}\rho U^2 \left(\dot{\mathbf{q}}^T \mathbf{A}_s \mathbf{q} + \frac{b}{U} \dot{\mathbf{q}}^T \mathbf{A}_d \dot{\mathbf{q}} \right) dt = \sum_{i=1}^{N} \sum_{j=1}^{N} (\Delta E_{d_{ij}} + \Delta E_{s_{ij}}) \tag{8}$$

$$\Delta E_{d_{ij}} = \frac{1}{4}\rho U^2 \pi |\Phi|_i |\Phi|_j (A_{d_{ij}} + A_{d_{ji}}) k \cos(\varphi_i - \varphi_j) \tag{9}$$

$$\Delta E_{s_{ij}} = -\frac{1}{4}\rho U^2 \pi |\Phi|_i |\Phi|_j (A_{s_{ij}} - A_{s_{ji}}) \sin(\varphi_i - \varphi_j) \tag{10}$$

where $\Delta E_{d_{ij}} = \Delta E_{d_{ji}}$ and $\Delta E_{s_{ij}} = \Delta E_{s_{ji}}$ = contributions of the aerodynamic damping and stiffness coupling between ith and jth structural modes, respectively; N = the total modal number.

The maximum potential energy of the system can be expressed as

$$E = \sum_{i}^{N} \sum_{j}^{N} |\Phi|_i |\Phi|_j (K_{ij} - \frac{1}{2}\rho U^2 A_{s_{ij}}) \cos(\varphi_i - \varphi_j) \tag{11}$$

Accordingly, the logarithmic aerodynamic damping ratio is given by

$$\delta = 2\pi\xi = -\Delta E/(2E) = \sum_{i=1}^{N} \sum_{j=1}^{N} (\delta_{d_{ij}} + \delta_{s_{ij}}) \tag{12}$$

$$\delta_{d_{ij}} = -\Delta E_{d_{ij}}/(2E); \quad \delta_{s_{ij}} = -\Delta E_{s_{ij}}/(2E) \tag{13}$$

where $\delta_{d_{ij}} = \delta_{d_{ji}}$ and $\delta_{s_{ij}} = \delta_{s_{ji}}$ = contribution to the aerodynamic damping due to aerodynamic damping coupling and stiffness coupling between ith and jth structural modes, respectively.

Fig. 3 shows the flutter motion in terms of the participation of structural modes with different amplitudes and phase angles. Fig. 4 shows the aerodynamic damping associated with the coupling among bridge modes at the critical flutter velocity of 68.9 m/s when modes 2, 8, 9, 10 and 11 were considered in analysis. For instance, the terms (2,2) represent the damping when the bridge is vibrating in the single mode 2. The term (2,10) indicates the damping attributed to the cross-terms of $\mathbf{A}_s$ and $\mathbf{A}_d$ relevant to modes 2 and 10. The summation of all these terms plus structural damping equal to zero at critical flutter velocity. Obviously, the two fundamental modes, modes 2 and 10, are most important modes in coupled flutter while other modes have secondary contributions. The large amplitudes of modes 8 and 9 are due to their resonance to coupled motion as their frequencies are close to the flutter frequency, while their contributions to aerodynamic damping are relatively small. The important role of the two fundamental modes in coupled flutter has been demonstrated by many flutter analysis examples. Therefore, the bimodal coupled flutter analysis that involves only the two fundamental modes remains a sufficiently accurate and useful tool for quickly evaluating bridge flutter performance at preliminary design stage, specially for seeking best bridge deck sections with superior aerodynamic characteristics. The spring-mounted bridge section model tests in wind tunnels developed since the investigation of Tacoma Narrows collapse continues to serve as a useful tool for estimating critical flutter velocity without the need to quantify the flutter derivatives.

(a) Amplitude ratios

(b) Phase angles
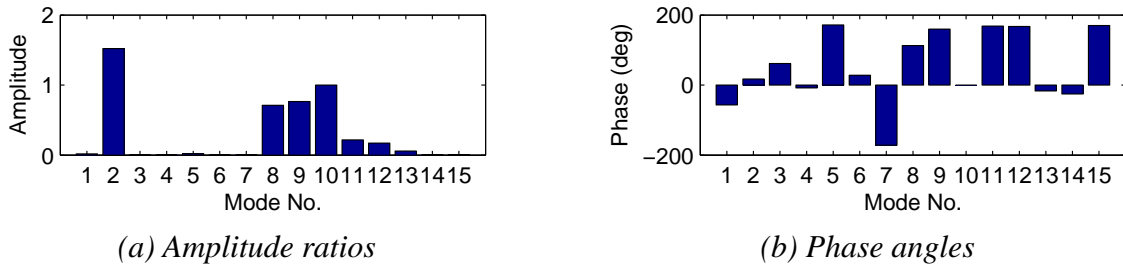
Fig. 3 Flutter motion in terms of participation of the structural modes (U=69.3 m/s)
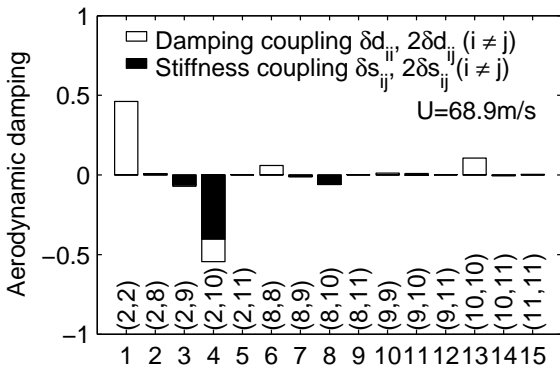
Fig. 4 Aerodynamic damping due to aerodynamic coupling among modes
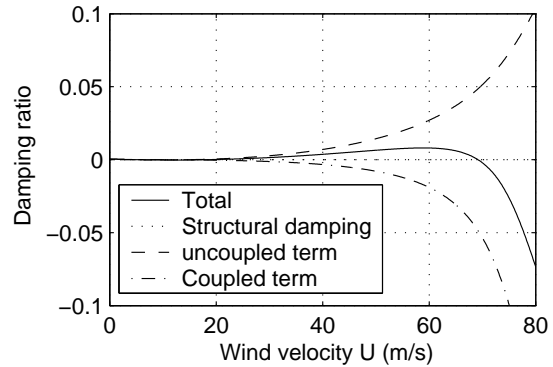
Fig. 5 Role of aerodynamic forces on modal damping of torsional branch (A bridge with a streamlined box section)

BIMODAL COUPLED FLUTTER

Improved understanding of the bimodal coupled flutter promises to gain insights to multimode coupled flutter. When only the two fundamental modes are considered, the dynamic displacements of the bridge deck in vertical direction and torsion are given as $h(x,t) = h_1(x)q_1(t)$ and $\alpha(x,t) = \alpha_2(x)q_2(t)$, where $h_1(x)$ and $\alpha_2(x)$ are mode shapes, $q_1(t)$ and $q_2(t)$ are the generalized modal coordinates. The self-excited lift (downward) and pitching moment (nose-up) acting on the bridge deck section per unit length are given

by (Scanlan 1978)

$$L_{se}(t) = \frac{1}{2}\rho U^2(2b)\Big(kH_1^*\frac{\dot{h}}{U} + kH_2^*\frac{b\dot{\alpha}}{U} + k^2H_3^*\alpha + k^2H_4^*\frac{h}{b}\Big) \tag{14}$$

$$M_{se}(t) = \frac{1}{2}\rho U^2(2b^2)\Big(kA_1^*\frac{\dot{h}}{U} + kA_2^*\frac{b\dot{\alpha}}{U} + k^2A_3^*\alpha + k^2A_4^*\frac{h}{b}\Big) \tag{15}$$

where H_j^* and A_j^* ($j = 1, 2, 3, 4$) = flutter derivatives which are functions of reduced frequency.

The aerodynamic matrices $\mathbf{A}_s(k)$ and $\mathbf{A}_d(k)$ for bimodal coupled system are expressed as

$$\mathbf{A}_s(k) = (2k^2)\left[\begin{array}{cc} H_4^*G_{h_1h_1} & bH_3^*G_{h_1\alpha_2} \\ bA_4^*G_{h_1\alpha_2} & b^2A_3^*G_{\alpha_2\alpha_2} \end{array}\right]; \quad \mathbf{A}_d(k) = (2k)\left[\begin{array}{cc} H_1^*G_{h_1h_1} & bH_2^*G_{h_1\alpha_2} \\ bA_1^*G_{h_1\alpha_2} & b^2A_2^*G_{\alpha_2\alpha_2} \end{array}\right] \tag{16}$$

where $G_{r_is_j} = \int_{\text{span}} r_i(x)s_j(x)dx$ (where $r, s = h, \alpha; i, j = 1, 2$) = modal integral.

While bimodal coupled flutter analysis can be carried out through Eq. (4), the framework with closed-form solutions presented in Chen and Kareem (2005) and Chen (2005a) offers more insight to the underlying physics of coupled flutter. Following this framework, the modal frequency and damping ratio of the torsional modal branch, and the associated amplitude ratio, Ψ, and phase difference between the vertical motion and torsion, ψ, as defined by $q_{10}/(bq_{20}) = \Psi e^{i\psi}$, are given by

$$\omega_2 = \omega_{s2}(1 + \upsilon A_3^* + \mu\upsilon D^2\Psi'\cos\psi')^{-1/2} \tag{17}$$

$$\xi_2 = \xi_{s2}\omega_{s2}/\omega_2 - 0.5\upsilon A_2^* - 0.5\mu\upsilon D^2\Psi'\sin\psi' \tag{18}$$

$$\Psi = \mu D R_{d2}\{[(H_3^*)^2 + (H_2^*)^2][G_{\alpha_2\alpha_2}/G_{h_1h_1}]\}^{1/2} \tag{19}$$

$$\psi = \tan^{-1}(H_2^*/H_3^*) - \tan^{-1}\{2\bar{\xi}_1'\omega_2/\bar{\omega}_1/[1 - (\omega_2/\bar{\omega}_1)^2]\} \tag{20}$$

where

$$R_{d2} = (\omega_2/\omega_1)^2\{\sqrt{[1 - (\omega_2/\bar{\omega}_1)^2]^2 + (2\bar{\xi}_1'\omega_2/\bar{\omega}_1)^2}\}^{-1/2} \tag{21}$$

$$\Psi' = R_{d2}\{[(H_3^*)^2 + (H_2^*)^2][(A_4^*)^2 + (A_1^*)^2]\}^{1/2} \tag{22}$$

$$\psi' = \tan^{-1}(A_1^*/A_4^*) + \psi \tag{23}$$

$$\bar{\omega}_1 = \omega_{s1}[1 - \mu(\omega_2/\omega_{s1})^2H_4^*]^{1/2} \tag{24}$$

$$\bar{\xi}_1' = \xi_{s1}\omega_{s1}/\bar{\omega}_1 - 0.5\mu(\omega_2/\bar{\omega}_1)H_1^* - \xi_2\omega_2/\bar{\omega}_1 \tag{25}$$

$\mu = \rho b^2/m$; $\upsilon = \rho b^4/I$; $m = m_1/G_{h_1h_1}$ and $I = m_2/G_{\alpha_2\alpha_2} = mr^2$= effective mass and polar moment of inertia per unit span, respectively; r = the radius of gyration of the bridge cross-section.

While iterative calculations for modal frequencies and damping ratios are required, these converge rapidly and even can be eliminated when their values at lower wind velocity are utilized as the initial values of calculations. The only assumption made in this framework is low level of system damping. This assumption is by no means restrictive. Therefore, as illustrated by many examples, this framework is expected to be applicable to bridges with a variety of deck sections.

In the case of well separated modal frequencies, the damping ratio of the torsional modal branches can be further simplified as

$$\xi_2 = \xi_{s2}\omega_{s2}/\omega_{20} - 0.5\upsilon A_2^* + 0.5\mu\upsilon D^2(H_3^*A_1^* + H_2^*A_4^*)/[1 - (\omega_{10}/\omega_{20})^2] \tag{26}$$

where ω_{10} and ω_{20} are the modal frequencies of the corresponding uncoupled system:

$$\omega_{10} = \omega_{s1}(1 + \mu H_4^*)^{-1/2}; \quad \omega_{20} = \omega_{s2}(1 + \upsilon A_3^*)^{-1/2} \tag{27}$$

This framework helps to better understand the development of coupled motions. The generation of coupled vertical motion in the torsional branch with a frequency ω_2 can be interpreted as follows. The

torsional motion causes lift force with an amplitude proportional to $\omega_2^2\sqrt{(H_2^*)^2 + (H_3^*)^2}$ and a phase angle $\tan^{-1}(H_2^*/H_3^*)$, indicating that this lift force leads the torsional displacement. This lift force, as an input of a single degree of freedom (SDOF) system which has a frequency $\bar{\omega}_1$ and damping ratio $\bar{\xi}_1'$, generates an output of vertical motion. This vertical motion lags the lift force by the angle $\theta_{d2} = \tan^{-1}\{2\bar{\xi}_1'\omega_2/\bar{\omega}_1/[1 - (\omega_2/\bar{\omega}_1)^2]\}$, which is function of frequency ratio $\omega_2/\bar{\omega}_1$ and damping ratio $\bar{\xi}_1'$. As $\omega_2/\bar{\omega}_1 > 1$, θ_{d2} is between $\pi/2$ and π, and will be very close to π for the system with well separated modal frequencies and low level of damping. Similar discussion can be made for the vertical modal branch. Detailed studies on $\tan^{-1}(H_2^*/H_3^*)$ for a number of slender bridge sections have indicated that the flutter modal branch corresponds to a coupled motion in which the torsional motion lags vertical motion.

The proposed framework also explicitly unveil the role of different aerodynamic force components on modal damping. The uncoupled aerodynamic forces, i.e., the lift caused by vertical motion and the pitching moment caused by torsion in terms of H_1^*, H_4^*, A_2^* and A_3^*, result in positive damping to both modal branches. The contribution of the coupled forces, i.e., the lift caused by torsion and the pitching moment caused by vertical motion in terms of H_2^*, H_3^*, A_1^* and A_4^*, to the torsional modal branch damping, depend on the arithmetic sign of $\sin\psi'$, where $\psi' = \tan^{-1}(H_2^*/H_3^*) + \tan^{-1}(A_1^*/A_4^*) - \theta_{d2}$. Based on the values of flutter derivatives of slender bridge sections, it is seen that the coupled self-excited forces produce a negative damping to the torsional modal branch, but a positive damping to the vertical modal branch. Fig. 5 shows the role of aerodynamic forces on torsional modal branch damping of a long span suspension bridge with a streamlined box section. When the negative aerodynamic damping exceeds the positive aerodynamic and structural damping, bridge becomes negatively damped which leads to the occurrence of flutter instability. The critical flutter velocity of this bridge is 69.1 m/s when the structural damping was neglected.

The role of coupled self-excited forces on modal damping can also be observed from the simplified formulation given by Eq. (26). For general slender bridge sections, $(H_3^*A_1^* + H_2^*A_4^*)$, is dominated by the value of $H_3^*A_1^*$, and is negative valued. Accordingly, the coupled self-excited forces produce negative damping to the torsional modal branch as $\omega_{10}/\omega_{20} < 1$. The significance of structural characteristics on bridge flutter can also be clearly identified from the proposed framework. This provides a critical insight to improved understanding of coupled flutter which lends itself to better tailoring of bridge systems for superior flutter performance.

ESTABLISHING RELATIONSHIP BETWEEN FLUTTER AND BUFFETING

The analysis of multimode coupled buffeting is often carried out in the frequency domain by spectral analysis. The power spectral density (PSD) matrix of $\mathbf{q}$, and the PSD function of any response component of interest (e.g., displacement, acceleration, and member force), $v = \mathbf{D}^T\mathbf{q}$, are expressed as

$$\mathbf{S_q}(\omega) = \mathbf{H_q}^*(\omega)\mathbf{S_{Q_b}}(\omega)\mathbf{H_q}^T(\omega); \qquad S_v(\omega) = \mathbf{D}^T\mathbf{S_q}(\omega)\mathbf{D} \tag{28}$$

$$\mathbf{H_q}(\omega) = \left(-\omega^2\mathbf{M} + i\omega\mathbf{C}_1(k) + \mathbf{K}_1(k)\right)^{-1} \tag{29}$$

$$\mathbf{S_{Q_b}}(\omega) = (\frac{1}{2}\rho U^2)^2\left(\mathbf{A}_{bu}^*(k)\mathbf{S_u}(\omega)\mathbf{A}_{bu}^T(k)/U^2 + \mathbf{A}_{bw}^*(k)\mathbf{S_w}(\omega)\mathbf{A}_{bw}^T(k)/U^2\right) \tag{30}$$

where $\mathbf{S_{Q_b}}(\omega)$, $\mathbf{S_u}(\omega)$ and $\mathbf{S_w}(\omega)$ = power spectral density matrices of $\mathbf{Q}_b$, $\mathbf{u}$ and $\mathbf{w}$, respectively; $\mathbf{D}$ = modal participation coefficients to response v; $\mathbf{H_q}$ = complex frequency response matrix/transfer matrix; Superscript T denotes matrix transpose operator. While the cross-power spectra between longitudinal and vertical wind fluctuations are neglected in Eq. (30), those can be readily included in a straightforward manner. The mean square value of the response is then quantified by integrating its power spectrum over the frequency range. The expected maximum response is determined by its root-mean-square (RMS) value multiplied by a peak factor which usually ranges between 3 and 4.

It is emphasized that while this currently used buffeting analysis framework is straightforward, it offers less information on how the complex modal properties affect the buffeting response. The determination of $\mathbf{H_q}(\omega)$ by Eq. (29) involves inverse of complex-valued matrix over a frequency range that demand considerable amount of computation. A unified framework for buffeting analysis is presented in Chen

(2005b), in which the transfer matrix is directly expressed in terms of the complex modal properties obtained from the flutter analysis. This framework establishes a clear nexus between bridge flutter and buffeting response and is simpler and illustrative.

This unified framework is based on the observation that the frequency response matrix and response spectra generally have very high peaks in close proximity of modal frequencies. Subsequently, the integration of response spectra in close neighborhoods of modal frequencies dominates the response variance and covariance. Within the vicinity of each modal frequency, the frequency dependent aerodynamic stiffness and damping terms can be approximately regarded as constants by taking their values at the modal frequency. This approximation is generally acceptable because it is applied only in a very small range of frequency, and also the aerodynamic parameters rarely markedly vary with frequency. Subsequently, the frequency response matrix can be approximately expressed in terms of the complex modal properties as (Chen 2005b):

$$\mathbf{H_q}(\omega) = \sum_{j=1}^{N} \left(\frac{\mathbf{\Phi}_j \mathbf{\Theta}_j^T / m_j}{i\omega - \lambda_j} + \frac{\mathbf{\Phi}_j^* \mathbf{\Theta}_j^{*T} / m_j}{i\omega - \lambda_j^*} \right) = \sum_{j=1}^{N} H_{j0}(\omega) \Big((i\omega)\mathbf{E}^j + \mathbf{F}^j \Big) \tag{31}$$

$$\mathbf{E}^j = (\mathbf{\Phi}_j \mathbf{\Theta}_j^T + \mathbf{\Phi}_j^* \mathbf{\Theta}_j^{*T}); \quad \mathbf{F}^j = -(\mathbf{\Phi}_j \mathbf{\Theta}_j^T \lambda_j^* + \mathbf{\Phi}_j^* \mathbf{\Theta}_j^{*T} \lambda_j) \tag{32}$$

$$H_{j0}(\omega) = \frac{1}{m_j(\omega_j^2 - \omega^2 + i2\xi_j \omega_j \omega)} \tag{33}$$

where $\mathbf{\Theta}_j$ = the eigenvector (mode shape) of the transpose of system matrix associated with λ_j:

$$\mathbf{\Theta}_j^T \Big(\lambda_j^2 \mathbf{M} + \lambda_j \mathbf{C}_1(k_j) + \mathbf{K}_1(k_j) \Big) = \mathbf{0} \tag{34}$$

and is normalized as

$$\mathbf{\Theta}_j^T \Big(2\lambda_j \mathbf{M} + \mathbf{C}_1(k_j) \Big) \mathbf{\Phi}_j = m_j \tag{35}$$

This new scheme is not only computationally more effective than the traditional framework which requires inverse of the complex matrix at discrete frequencies [Eq (29)], but also sheds more physical insight to bridge aeroelastic response by explicitly linking the effects of the self-excited and buffeting forces. The self-excited forces affect the modal properties of the system thus influence the way bridge responds to wind fluctuations. Obviously, when wind velocity exceeds the critical flutter velocity, the contribution of flutter mode becomes infinite, thus system turns to be unstable.

Fig. 6 compares the RMS values of the deck displacements of a long span suspension bridge predicted based on the two different approaches. The results indicated by "Exact" are based on the traditional approach in which $\mathbf{H_q}(\omega)$ is directly evaluated using Eq. (29). The results denoted by "Approx." represent those based on Eq. (31). These results illustrated the accuracy of the proposed scheme.

(a) Lateral　　　　　　*(b) Vertical*　　　　　　*(c) Torsional*
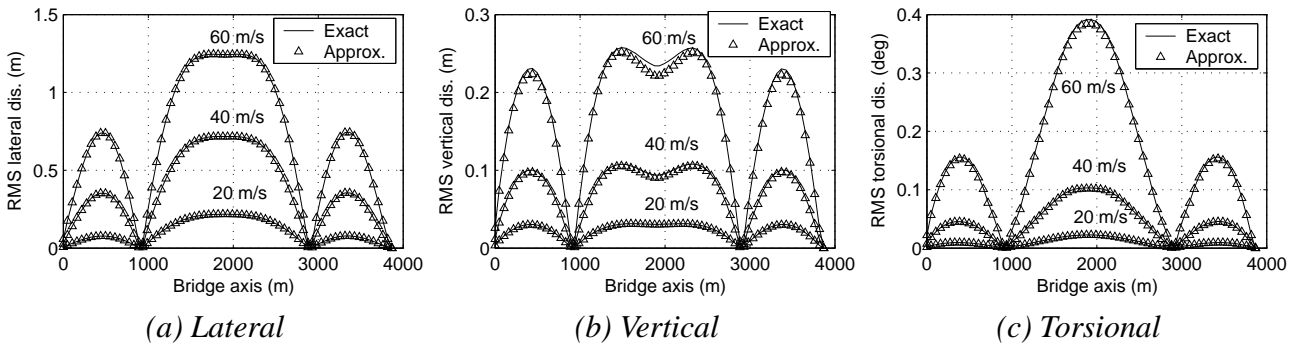
Fig. 6 The RMS values of bridge deck displacements

This framework also permits time domain simulation of multimode coupled buffeting response. The modal response can be expressed in the frequency domain as

$$\mathbf{q}(\omega) = \mathbf{H_q}(\omega)\mathbf{Q}_b(\omega) = \sum_{j=1}^{N}\left((i\omega)\mathbf{E}^j\mathbf{Y}^j(\omega) + \mathbf{F}^j\mathbf{Y}^j(\omega)\right) \tag{36}$$

$$\mathbf{Y}^j(\omega) = H_{j0}(\omega)\mathbf{Q}_b(\omega) \tag{37}$$

Consequently, the generalized displacement can be expressed in the time domain as

$$\mathbf{q}(t) = \sum_{j=1}^{N}\left(\mathbf{E}^j\dot{\mathbf{Y}}^j(t) + \mathbf{F}^j\mathbf{Y}^j(t)\right) \tag{38}$$

where $\mathbf{Y}^j(t)$ is given as follows for its element $Y_n^j(t)$ $(n = 1, 2, ..., N)$:

$$\ddot{Y}_n^j(t) + 2\xi_j\omega_j\dot{Y}_n^j(t) + \omega_j^2 Y_n^j(t) = Q_n(t) \tag{39}$$

This framework can be used for time domain simulation of buffeting response without generating time histories of self-excited forces. The influence of self-excited forces on buffeting response is accounted through the complex modal properties. The time histories of buffeting forces can be either generated based on their spectra or calculated based on the time histories of wind fluctuations. In the later format, the rational function approximation technique can be utilized to model the frequency dependent features of the unsteady buffeting forces instead of using quasi-steady assumption (Chen and Kareem 2000b and 2002). The time domain simulation technique with generation of time histories of self-excited and buffeting forces is more appropriate when aerodynamic nonlinearities are taken into consideration (Chen and Kareem 2003).

EQUIVALENT STATIC WIND LOAD

The equivalent static wind loading representation is very effective for extracting design wind loads on bridges from full aeroelastic and/or section model wind tunnel tests. The equivalent static wind loads associated with multimode coupled buffeting response can be expressed in terms of the modal inertial loads, which are a function of structural mass distribution, mode shape and modal accelerations (Davenport and King 1984; Irwin 1998; Holmes 1999; Chen and Kareem 2001). It provides physically more meaningful design loads than the traditional gust response factor approach that results in a load distribution similar to the mean wind loads.

The bridge dynamic displacement in the vertical, lateral and torsional direction $h(x,t), p(x,t)$ and $\alpha(x,t)$, respectively, are expressed as

$$h(x,t) = \sum_j h_j(x)q_j(t); \quad p(x,t) = \sum_j p_j(x)q_j(t); \quad \alpha(x,t) = \sum_j \alpha_j(x)q_j(t) \tag{40}$$

where $h_j(x), p_j(x)$ and $\alpha_j(x) = j$th mode shapes in the vertical, lateral and torsional directions, respectively; and x = the spanwise position.

The lift, drag and pitching moment components of the equivalent static modal load associated with the jth mode are given in terms of modal inertial loads as

$$L_{ej}(x) = m(x)h_j(x)\omega_{js}^2\sigma_{q_j}; \quad D_{ej}(x) = m(x)p_j(x)\omega_{js}^2\sigma_{q_j}; \quad M_{ej}(x) = I(x)\alpha_s(x)\omega_{js}^2\sigma_{q_j} \tag{41}$$

where $m(x)$ and $I(x)$ = mass and rotational inertia per unit length, respectively; σ_{q_j} = RMS value of q_j.

The equivalent static load for a given peak response can be expressed in terms of linear combinations of these modal inertial loads as

$$L_e(x) = g\sum_{j=1}^{N}L_{ej}(x)W_j; \quad D_e(x) = g\sum_{j=1}^{N}D_{ej}(x)W_j; \quad M_e(x) = g\sum_{j=1}^{N}M_{ej}(x)W_j \tag{42}$$

where W_j = weighting factor or combination factor.

For instance, for an arbitrary dynamic response of interest $z(t)$ (e.g., bending moment, shear force, and other member forces), its expected peak value is estimated as

$$z_{max} = g\sigma_z = g\left(\sum_j \sum_k \Gamma_j \Gamma_k \sigma_{q_j} \sigma_{q_k} r_{jk}\right)^{1/2} \tag{43}$$

and the weighting factor of the jth modal inertial load is given by

$$W_j = \sum_k r_{jk} \rho_k \sigma_{q_k}/\sigma_z \tag{44}$$

where g = the peak factor, generally in the range 3 to 4; $r_{jk} = r_{kj} = \sigma_{q_{jk}}^2/(\sigma_{q_j}\sigma_{q_k})$ and $\sigma_{q_{jk}}^2$ = the correlation coefficient and covariance between jth and kth modal responses; $\Gamma_j = j$th modal participation coefficient.

In fact, there are many ways to define the weighting factor hence the equivalent static load for a given peak response, but Eqs. (42) and (44) is based on the load-response-correlation approach and provides the most probable peak load distribution for the specified maximum response (Kasperski 1992). The equivalent static load distributions depend on the influence function of the specific response and are unique for each response component. It is also worth noting that only the relative value of the influence function is needed for determining these weighting factors.

The dynamic displacement response can be quantified through a full aeroelastic model test. Using this equivalent static load approach, full bridge aeroelastic model test not only can be used as a final confirmation of the performance of an important bridge, but can also be used to gain useful insight into the description of the design wind loads (King 1999).

A long span suspension bridge with a main span of approximately 2000 m is considered as an example to illustrate the aforementioned methodology. The buffeting displacement is predicted based on a three-dimensional multimode coupled buffeting analysis. First fifteen natural modes with the frequencies over the range of 0.03 to 0.2 Hz are included in the analysis.

Bending moments in lateral and vertical directions, and the displacement in torsion at the main span center at the mean wind speed of 60 m/s are selected as the response components of interest for the equivalent static loads. Fig. 7 shows the corresponding equivalent static load distributions. The peak factor was assumed to be 3.5. It is clear that for different response components the equivalent static load distributions are different. It is also shown that the aerodynamic coupling has a significant influence on the equivalent static load distribution. For potential application in design practice, it is necessary to limit the number of distributions to only critical response components and to simplify the mode shapes for a convenient description of the load distributions.
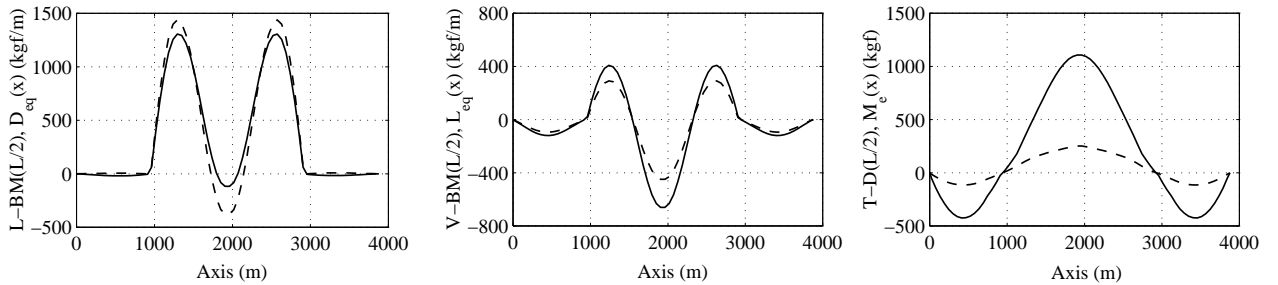
Fig. 7 Equivalent Static load distribution for different response
(U=60m/s ; —— w/ coupling; - - w/o coupling)

CONCLUDING REMARKS

This paper discussed a number of useful analysis frameworks recently developed at the authors' laboratories, which offer advanced prediction and a clearer explanation of the multimode coupled bridge response

to strong wind excitations. By exploring the contribution of bridge modal coupling to flutter modal damping through the viewpoint of energy change during a cycle of vibration, the important role of the fundamental vertical and torsional modes in flutter was identified. This also pointed out the consistency in the underlying physics of the multimode coupled flutter with the bimodal coupled flutter, and confirmed the usefulness of bimodal coupled flutter analysis for an expeditious assessment of bridge aerodynamic performance. The framework with closed-form solutions for bimodal coupled system provided enhanced understanding of the generation of coupled motion and the evolution of flutter, and offered insights to how and where the structure be modified for tailoring of better flutter performance. The proposed framework for buffeting analysis explicitly integrated the aeroelastic modal information, e.g., aerodynamic damping and inter-modal coupling, gained through flutter analysis, and is indeed more illustrative. This has helped to better understand the role of both self-excited and buffeting forces on the buffeting response. Finally, the modeling of equivalent static loading provided a useful tool for extracting underlying design wind loads on bridges experiencing multimode coupled dynamic response to strong winds.

ACKNOWLEDGMENT

REFERENCES

Chen, X. (2005a). "Some observations on coupled bridge flutter." *J. of Eng. Mech.*, ASCE (in preparation).

Chen, X. (2005b). "Analysis of long span bridge response to wind: Building nexus between flutter and buffeting." *J. of Struct. Eng.*, ASCE (in preparation).

Chen, X. and Kareem, A. (2005). "Revisiting multimode coupled bridge flutter: some new insights. *J. of Eng. Mech.*, ASCE (under review).

Chen, X. and Kareem, A. (2003). "Aeroelastic analysis of bridges: turbulence effects and aerodynamic nonlinearity." *J. of Eng. Mech.*, ASCE,, 129(8), 885-895.

Chen, X. and Kareem, A. (2002). "Advances in modeling of aerodynamic forces on bridge decks." *J. of Eng. Mech.*, ASCE, 1193-1205.

Chen, X. and Kareem, A. (2001). "Equivalent static loads for buffeting response of bridges. " *J. of Struct. Eng.*, ASCE, 127(12),1467-1475.

Chen, X., Matsumoto, M. and Kareem, A. (2000a). "Aerodynamic coupling effects on flutter and buffeting of bridges." *J. of Engrg. Mech.*, ASCE, 126(1), 17-26.

Chen, X., Matsumoto, M. and Kareem, A. (2000b). "Time domain flutter and buffeting response analysis of bridges." *J. of Engrg. Mech.*, ASCE, 126(1), 7-16.

Davenport, A. G. and King, J. P. C. (1984). "Dynamic wind forces on long span bridges." *Proc. of 12th IABSE Congress*, Vancouver, Canada.

Diana, G., Cheli, F., Zasso, A. and Bocciolone, M. (1999) "Suspension bridge response to turbulent wind: comparison of new numerical simulation method results with full scale data." *Proc. of the 10th Int. Conf. on Wind Eng.*,, Copenhagen, Denmark; *Wind Engineering into 21st Century*, Larsen, Larose & Livesey (eds), Balkema, Rotterdam, The Netherlands, 871-878.

Holmes, J. D. (1999). "Equivalent static load distributions for resonant dynamic response of bridges." *Proc. of the 10th Int. Conf. on Wind Eng.*,, Copenhagen, Denmark; *Wind Engineering into the 21st Century*, Larsen, Larose & Livesey (eds), Balkema, Rotterdam, The Netherlands, 907-911.

Irwin, P. A. (1998). "The role of wind tunnel modeling in the prediction of wind effects on bridges." *Bridge Aerodynamics*, Larsen & Esdahl (eds), Balkema, Rotterdam, The Netherlands, 99-117.

Kasperski, M. (1992). "Extreme wind load distributions for linear and nonlinear design." *Eng. Struct.*, 14, 27-34.

King, J. P. C. (1999). "Integrating wind tunnel tests of full aeroelastic models into the design of long span bridges." *Proc. of the 10th Int. Conf. on Wind Eng.,*, Copenhagen, Denmark; *Wind Engineering into the 21st Century*, Larsen, Larose & Livesey (eds), Balkema, Rotterdam, The Netherlands, 927-934.

Jones, N. P., Scanlan, R. H., Jain A. and Katsuchi, H. (1998). "Advances (and challenges) in the prediction of long-span bridge response to wind." *Bridge Aerodynamics*, Larsen & Esdahl (eds), Balkema, Rotterdam, The Netherlands, 59-85.

Matsumoto, M. (1999). "Recent study on bluff body aerodynamics and its mechanism." *Wind Engineering into the 21 Century*, Larsen, Larose & Livesey (eds), Balkema, Rotterdam, 67-78.

Miyata, T., Tada, K., Sato, H., Katsuchi, H., and Hikami, Y. (1994). "New findings of coupled flutter in full model wind tunnel tests on the Akashi Kaikyo Bridge." *Proc. of Symp. on Cable-Stayed and Suspension Bridges*, Deauville, France, October 12-15, 163-170.

Scanlan, R. H. (1978). "The action of flexible bridges under wind, I: flutter theory; II: buffeting theory." *J. of Sound and Vibration*, 60(2), 187-199; 201-211.